JOURNAL OF THE CIVIL ENGINEERING FORUM

Journal of Civil Engineering Forum, January 20XX, X(X): xx-xx
DOI 10.22146/jcef.XXXXX
Available Online at http: https://jurnal.ugm.ac.id/jcef/issue/archive

Best Fitting of The Mud Profile Equations

A.Perwira Mulia Tarigan[1*] and Hasanul Arifin Purba[1]
[1]Civil Engineering Department, Universitas Sumatera Utara

*a.perwira@usu.ac.id
[*]Corresponding authors: a.perwira@usu.ac.id

SUBMITTED xxxx REVISED xxxxx ACCEPTED xxxx

ABSTRACT In order to understand the dynamics of shoreline changes due to natural and anthropogenic causes, it is imperative that a coastal manager comprehend the shore profile characteristics which are dependent on the sediment-wave interaction and can be depicted in a profile equation. Based on the argument of wave energy dissipation per unit bed area and unit time, the power form of the profile equation for a sandy coast can be derived. Using the same argument and considering the phenomenon that the main cause of wave damping over a muddy coast is due to energy absorption by the soft mud bottom, the mud profile equation can be formulated. In this study, shore profile data measured from the muddy coast of Pantai Cermin, a muddy shore on the eastern coast of North Sumatera Province, are fitted to both the sand and mud profile equations. The procedures and results of two best fitting methods, the nonlinear regression and the least square based trial and error search, are exhibited and compared. Several noteworthy features of the mud profile equation are shown as compared to that of the sand profile equation in describing the profile data.

KEYWORDS Best fitting; shore profile; mud profile; sand profile

1 INTRODUCTION

A shore profile would result from nearshore forces acting on the bed sediments across the active sediment mobility zone. The sediments composing the coast may in general consist of mud or sand. In an episode of stormy weather conditions, the bed sediments would interact with waves, the typically predominant forces in an open coast, in a way that would dissipate the wave energy and result in a (dynamic) equilibrium profile (Dean and Dalrymple, 2002).

It has been commonly recognized that the main wave energy dissipation over a sandy coast is due to turbulent breaking mechanism across the surf zone. In contrast, over a muddy coast, the wave energy is damped due to the existence of soft, mud bottom (Tarigan, 1996; Tarigan, 2002). The resulting mud profiles are typically milder and most plausibly longer than the sandy profiles. Hence the mud profile equations proposed should also different and reflect their distinctive characters.

The objective of this paper is to expose the geometry of the mud profile equations through best fitting the proposed equations to the field data. Based on the field data and observation, characteristic features of the mud profiles are then shown as opposed to that of sand profiles.

2 BACKGROUND THEORY

A shore profile is a geometry of the variation of water depth with distance perpendicularly offshore from the shoreline. The equilibrium shore profile is theoretically the result of balancing between the destructive and constructive forces acting across the profile. In nature since the incident wave field and water level change continuously, the equilibrium profile should be considered to be a dynamic concept (Dean and Dalrymple, 2002).

The derivations of the following shore profile equation are based on the argument of wave energy conservation, i.e., if a profile composed of a given sediment size is considered to be able to withstand a given level energy dissipation per unit water volume or area, then the profile will respond dynamically toward the equilibrium shore profile.

2.1 Sand Profile Equations

Bruun (1954) and Dean (1977) are among the first who proposed a power form for a profile composed of coarse grained sediments.

$$h = Ay^n \tag{1}$$

where h = water depth (m), A = profile scale parameter, y = distance from shoreline (m) and n = constant. Dean (1977) found that the value of n = 2/3 can be derived from the argument of equilibrium beach profile resulting from wave energy dissipation per unit volume D_{eq} as follows:

$$D_{eq} = \frac{dP}{hdy} \tag{2}$$

The energy flux P can be expressed using the shallow water assumption of the linear wave theory as follows:

$$P = \frac{1}{8}\rho g H^2 \sqrt{gh} \tag{3}$$

where ρ = the density of the fluid. It should be noted that the main wave energy dissipation is due to turbulence generating breaking over the surf zone where the wave height can be written in terms of the breaking index k,

$$H = kh \tag{4}$$

The dissipation D_{eq} then becomes:

$$D_{eq} = \left[\frac{5}{16}\rho g^{2/3} k^2\right] h^{1/2} \frac{dh}{dy} \tag{5}$$

which can be solved to yield the sand profile equation:

$$h = Ay^{2/3} \tag{6}$$

The value of A is given as follows:

$$A = \left(\frac{24 D_{eq}}{5\rho g^{3/2} k^2}\right)^{3/2} \tag{7}$$

2.2 Mud Profile Equations

Mud profiles are generally located on low laying coastal areas, especially in the vicinities of estuaries where abundant fine sediments are suspended and dispersed toward the coastal waters. The muddy coasts with soft sediment bottom are typically broad, flat and shallow, forming mild profiles (Tarigan and Nurzanah, 2016).

Lee (1995) and Lee and Mehta (1997) argued that across the mud profile the breaking wave is not the main energy dissipation and stated that the thickness of the fluid mud affects the absorption of wave energy. For this reason, the wave damping is expressed as follows:

$$H_{(y)} = H_0 e^{-Ki(y_0 - y)} \tag{8}$$

where H_0 = the height of the incident wave at $y = y_0$, y_0 = the length of the active profile, and K_i = the wave damping coefficient. Next, this equation is substituted into a uniform wave energy dissipation equation per unit area E_{eq},

$$E_{eq} = \frac{d}{dy}\left(EC_g\right) \tag{9}$$

With shallow water condition $C_g = \sqrt{gh}$, Eq. 8 combined with Eq. 9 results in

$$\frac{\rho g^{3/2} H_0^2}{2} \frac{d}{dy}\left[e^{2K_i(y-y_0)}\sqrt{h}\right] = E_{eq} \quad (10)$$

The above equation is integrated from the coastline (0, 0) to the point (y, h) (Mehta, 2014)

$$\int_{0,0}^{y,h} d\left[e^{2K_i(y-y_0)}\sqrt{h}\right] = \int_0^y \frac{2E_{eq}}{\rho g^{3/2} H_0^2} dy \quad (11)$$

which can be solved as

$$e^{2\overline{k_l}(y-y_0)}\sqrt{h} = \frac{2E_{eq}}{\rho g^{3/2} H_0^2} y \quad (12)$$

where $\overline{k_l}$ represents the average wave damping coefficient. This expression should satisfy the boundary condition, i.e., $h = h_0$ at $y = y_0$. So that

$$H_0^2 = \frac{2_{Eq} y_0}{\rho g^{3/2} \sqrt{h_0}} \quad (13)$$

Subsituting Eq. 13 to Eq. 12 yields the initial mud profile equation

$$h = h_0 e^{4\overline{k_l}(y_0-y)}\left(\frac{y}{y_0}\right)^2 \quad (14)$$

Lee (1995) found that Eq. 14 did not match well with field data on the nearshore of the profile and reasoned that the mechanism of wave dissipation other than that arising from the absorption of wave energy by mud, for example turbulence due to breaking waves, causes the discrepancy. To solve this problem, Lee (1995) added the correction term C_N to Eq. 14 to get h.

$$C_N = Fye^{-\beta y}$$

$$h = Fye^{-\beta y} + h_0 e^{4\overline{k_l}(y_0-y)}\left(\frac{y}{y_0}\right)^2 \quad (15)$$

where F = bottom slope at the shoreline and β = offshore extent of the combined influence of the slope at the shoreline and scour due to wave breaking. Finally, to maintain consistency at the boundary conditions, $h = h_0$ at $y = y_0$, Lee (1995) obtained the final shape for the mud profile geometry.

$$h = Fye^{-\beta y} + \left(h_0 - Fye^{-\beta y}\right)e^{4\overline{k_l}(y_0-y)}\left(\frac{y}{y_0}\right)^2 \quad (17)$$

He concluded that this geometry still retained the analytic properties of the model stated by Eq. 14.

In this study a different correction term C_N is suggested to improve the performance of the equation near the shoreline as follows.

$$C_N = F(1-e^{-\beta y}) \quad (18)$$

So Eq. 14 becomes

$$h = F(1-e^{-\beta y}) + h_0 e^{4\overline{k_l}(y_0-y)}\left(\frac{y}{y_0}\right)^2 \quad (19)$$

To maintain consistency at the boundary conditions, $h = h_0$ at $y = y_0$, the modified mud profile equation is obtained.

$$h = F(1-e^{-\beta y}) + (h_0 - Fye^{-\beta y})e^{4\overline{k_l}(y_0-y)}\left(\frac{y}{y_0}\right)^2 \quad (20)$$

2.3 Nonlinear Regression and Trial Error Method

The nonlinear regression method is based on the Gauss-Newton method and the Tayor series. The Gauss-Newton method is an algorithm to minimize the sum of squares of the difference between the data and the nonlinear equation. The key concept underlying this technique is that the Taylor series expansion is used to express the original nonlinear equation in a linear, approximate form. Then, the least-squares theory can be used to get new estimates of parameters aimed at minimizing residuals (Chapra and Canale, 2015).

To illustrate how this is done, first the relationship between nonlinear equations and data can be stated generally as

$$y_i = f(x_i; a_0, a_1, ..., a_m) + e_i \quad (21)$$

where y_i = the measured value of the dependent variable, $f(x_i; a_0, a_1, ..., a_m)$ = the equation which is a function of the independent variable x_i and the nonlinear function of the parameter $a_0, a_1, ..., a_m$ and e_i = a random error. For convenience, this model can be expressed in a simple form by eliminating parameters.

$$y_i = f(x_i) + e_i \quad (22)$$

The nonlinear model can be extended in the Taylor series around parameter values and limited up to the first derivative. For example, for the case of two parameters.

$$f(x_i)_{j+1} = f(x_i)_j + \frac{\partial f(x_i)_j}{\partial a_0}\Delta a_0 + \frac{\partial f(x_i)_j}{\partial a_1}\Delta a_1 \quad (23)$$

where j = initial value, j + 1 = prediction, $\Delta a_0 = a_{0,j+1} - a_{0,j}$ and $\Delta a_1 = a_{1,j+1} - a_{1,j}$. Then by subsituting Eq. 23 to Eq. 22 the following is obtained:

$$y_i - f(x_i)_j = \frac{\partial f(x_i)_j}{\partial a_0}\Delta a_0 + \frac{\partial f(x_i)_j}{\partial a_1}\Delta a_1 + ei \quad (24)$$

or in the matrix form:

$$\{D\} = [Z_j]\{\Delta\hat{A}\} + \{E\} \quad (25)$$

where $[Z_j]$ is the partial derivatif matrix of function that is evaluated at the initial value,

$$[Z_j] = \begin{bmatrix} \partial f_1/\partial a_0 & \partial f_1/\partial a_1 \\ \partial f_2/\partial a_0 & \partial f_2/\partial a_1 \\ . & . \\ \partial f_m/\partial a_0 & \partial f_m/\partial a_1 \end{bmatrix}$$ m = number of data, and $\partial f_i / \partial a_k$ = the partial derivative of the function with respect to the k-th parameter evaluated at the i-th data point. Vector {D} contains the difference between measurement and function value, $\{D\} = \begin{Bmatrix} y_1 - f_{(x_1)} \\ y_2 - f_{(x_2)} \\ . \\ : \\ y_m - f_{(x_m)} \end{Bmatrix}$ and vector $\{\Delta\hat{A}\}$ contains the difference of parameter value, $\{\Delta\hat{A}\} = \begin{matrix} \Delta a_0 \\ \Delta a_1 \\ . \\ : \\ \Delta a_m \end{matrix}$

Applying the theory of least squares to Eq. 25 produces the following normal equation:

$$\left[[Zj]^T [Zj]\right]\left\{\Delta\hat{A}\right\} = \left\{[Z_j]^T \{D\}\right\} \quad (26)$$

Thus, the approach consists of completing Eq. 26 for $\left\{\Delta\hat{A}\right\}$, which can be used to calculate the value of parameters, $\Delta a_{0,j+1} = a_{0,j} - \Delta a_0$ and $\Delta a_{1,j+1} = a_{1,j} - \Delta a_1$. This procedure is repeated until the solution converges, that is until the standard error reaches the value below an acceptable stopping criterion.

$$S = \sqrt{\frac{\sum (y_i - f_{(x_i)})^2}{m-1}} \quad (27)$$

The trial and error method is done by systematically changing (or increasing) the values of the parameters with a very small interval (for example 0.001) in the valid ranges considered. At each step of computation the standard error of Eq. 27 is calculated. The computation step which yields the smallest value of standard error *e* is identified and defined as the best solution containing the best parameters. Figure 1 shows the flowchart of the best fitting of the profile equation to the field data using the two methods described above.

3 FIELD SITE AND MEASUREMENT

The field site is on the muddy coast of Pantai Cermin, in the village of Kota Pari, the district of Pantai Cermin, and the county of Serdang Bedagai. The locals name the site as Pantai Mutiara, located on the eastern coast of North Sumatera Province, fronting the Strait of Malacca. It is about 43 km from Medan, the capital city of Sumatera Utara Province. The geographic location of the study area is in the vicinity of 3° 39' 46" northern latitude and 98° 57' 54" eastern longitude. Figure 2 shows the location of the field site.

The profile measurement was conducted using a geodetic GPS with the RTK (real time kinematic) method. The accuracy of the measurement can be obtained up to 5 mm in horizontal and vertical positions. The coordinates (*x*, *y*, *z*) were given in the UTM projection system on the zone of 47 N.

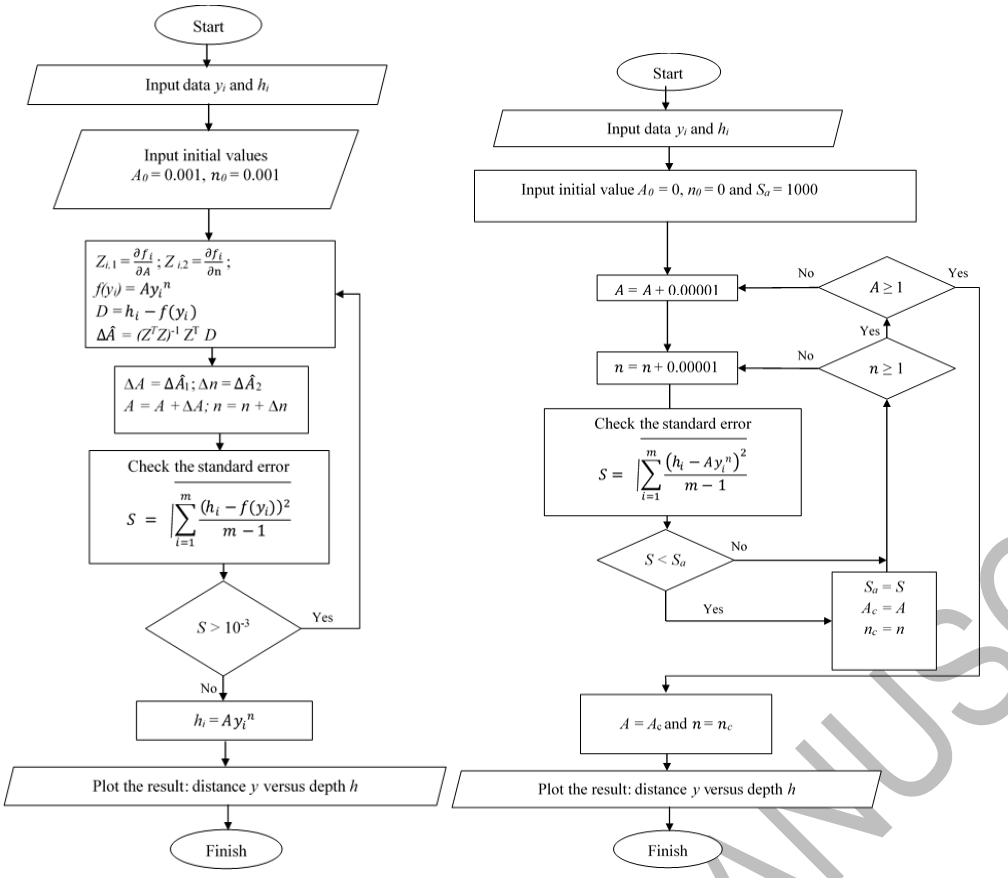

Figure 1. Flowchart of best fitting of the profile equation using (a) nonlinier regression and (b) trial and error methods

Figure 2. Location of the field site

Table 1 shows the field data in terms of distance from shoreline and elevation. Note that the minus sign indicates the point of measurement is already in the water with reference to the local datum which is approximately the mean high-water level.

Table 1. Field data

No.	Distance from shoreline y(m)	Elevation h(m)	No.	Distance from shoreline y(m)	Elevation h(m)
1	-46.443	0.487	11	28.490	-0.981
2	-30.895	0.596	12	57.947	-1.027
3	-12.432	1.388	13	86.417	-1.002
4	-8.498	1.379	14	162.321	-1.165
5	-4.438	0.638	15	223.429	-1.231
6	0.000	0.000	16	277.884	-1.342
7	1.294	-0.186	17	327.736	-1.494
8	5.262	-0.617	18	359.460	-1.591
9	8.663	-1.013	19	401.065	-1.701
10	16.998	-1.043			

4 RESULT AND DISCUSSION

Two methods are used to fit the profile equations with the field data, i.e. nonlinear regression and trial and error methods. The results of best fitting using both methods for the sand profile equation and the mud profile equations and are shown and compared in the following. Figure 3 shows the results for the sand profile equation, while Figure 4 shows the results for the mud profile equations.

The sand profile equation is fitted to two different sets of data, i.e. the beach face part and the whole part. Figure 3a shows the result of best fitting the sand profile equation with the beach face data using the nonlinear regression, whereas Figure 3b exhibits the result of the same equation with the same data using the trial and error method. It can be seen that both methods yield about the same order of accuracy. A noteworthy feature in these two figures is the fact that the sand profile equation can represent only on near the shoreline part of the profile data. It is in agreement with the field observation that the sand with median size of 0.5 – 1.00 mm is typically deposited on the beach face of the profile.

Figures 3c and 3d show the result of best fitting the sand profile equation with the whole data using nonlinear regression and trial and error methods, respectively. It can be seen, as noted in the previous case, that both methods give about the same order of accuracy. A noteworthy feature in these two figures is the fact that the value of n is very low compared with the suggested value n = 2/3. This indicates that the profile is very mild, especially on the main portion below the beach face where mud is typically deposited.

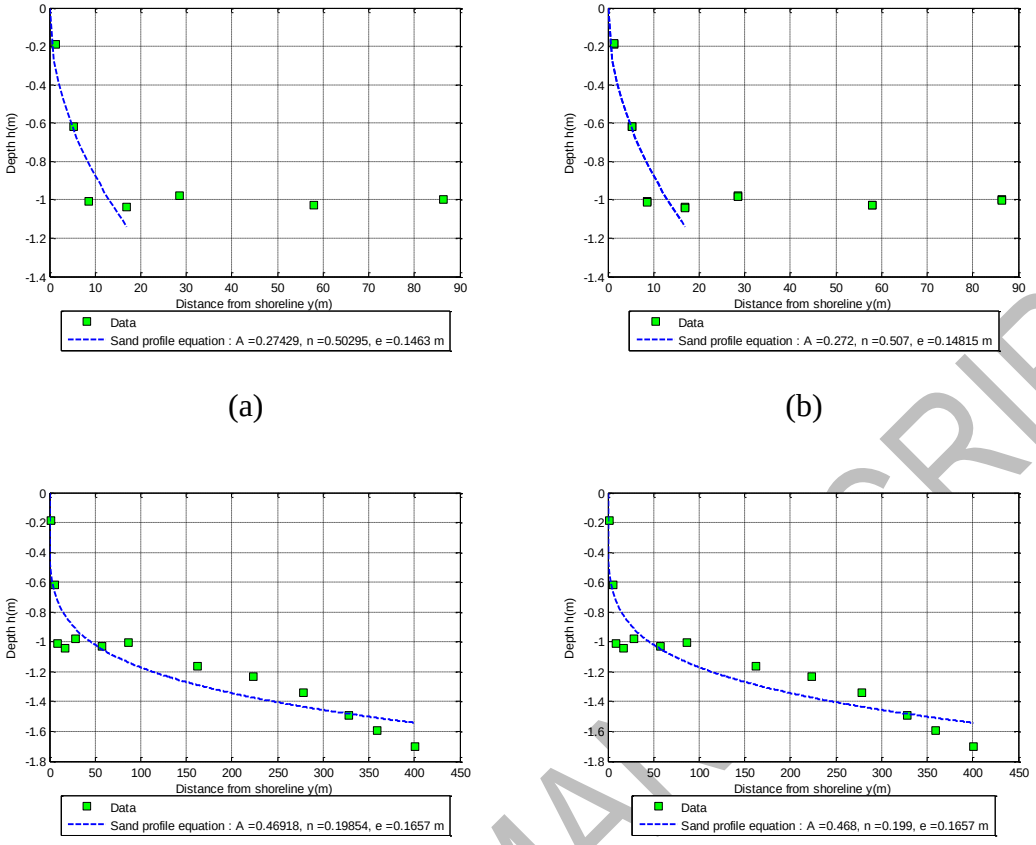

Figure 3. Results of best fitting of sand profile equation at the beach face using (a) nonlinear regression and (b) trial and error methods and with all of field data using (c) nonlinear regression and (d) trial and error methods

Figures 4a and 4b show the result of best fitting the mud profile equation of Eq. 17 with the whole data using nonlinear regression and trial and error methods, respectively. It can be seen that the nonlinear regression yields a slightly better accuracy. However, both methods exhibit the discrepancy significantly noticed near the shoreline. This suggests that the mud profile equation of Eq. 17 has a drawback in characterizing the beach face. This drawback is then improved in Figures 4c and 4d in which the results of best fitting the mud profile equation of Eq. 20 with the whole data using nonlinear regression and trial and error methods are given respectively. As indicated by the lowest standard errors, the mud profile equation of Eq. 20 has performed the best in fitting with the mud profile data. It should be noted that in doing the best fitting, one has to be aware of the ranges of the values valid for the parameters F, β and $\bar{k}_i$.

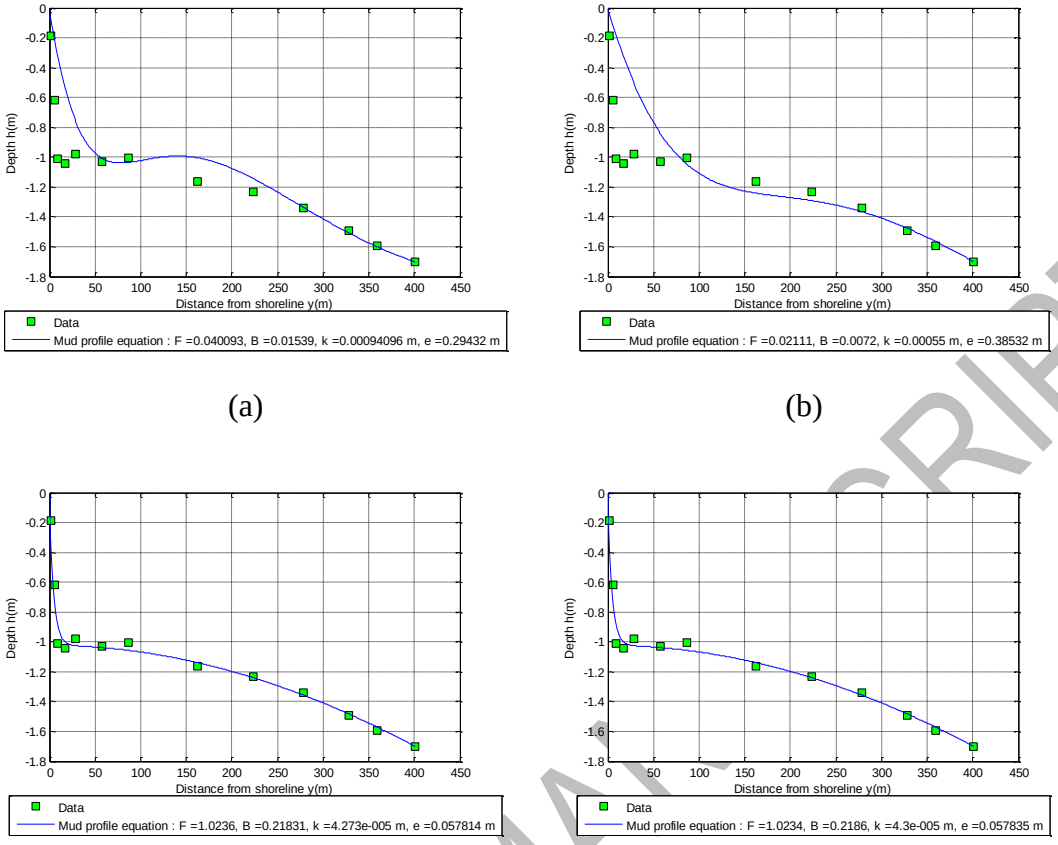

Figure 4. Results of best fitting of the mud profile equation of Eq. 17 using (a) nonlinear regression and (b) trial and error methods and best fitting of Eq. 20 using (c) nonlinear regression and (d)trial and error methods

5 CONCLUSION

Based on the results on discussion above the following points of conclusion can be stated:

1) Both method of nonlinear regression and trial and error methods yield about the same accuracy. In order to perform the best fit, one has to be aware of the ranges of the values valid for the parameters involved.
2) The sand profile equation is good only for the beach face part of the profile where sand is typically deposited.
3) The mud profile is so mild that the n value of the sand profile equation, suggested commonly to be n = 2/3, is meaningless.
4) The mud profile equation of Eq. 17 suggested by Lee (1995) is derived based on the assumption of wave damping due the existence of soft, mud bottom, a characteristic feature different from that of the sand profile equation. However it performed troublesomely on the foreshore part of the profile.
5) The modified mud profile equation of Eq. 20 improves the drawback of Eq. 17 and yields the best fitting with the whole data, including the steep foreshore of the profile.

It is recommended that more profile data be obtained to examine the applicability of the mud profile equations. The knowledge of shore profiles shall be essential to a coastal manager who deals with profile and shoreline stabilization.

DISCLAIMER

The authors declare no conflict of interest.

ACKNOWLEDGMENTS

The authors express their profound gratitude's and thanks to the Tourist Agency of Yogyakarta Province for providing information regarding the history of the ancient history of the Mataram Canal Development, and to the

SerayuOpak River Basin for providing related report and discussion regarding the operation and maintenance of Mataram Canal.

REFERENCES

Baolis (Step Wells) of Delhi, https://rangandatta.wordpress.com/20170510/baolis-step-wells-of-delhi, downloaded on 27 September 2019

Baolis of Mehrauli, https://en.wikipedia.org/wiki/Baolis_of_Mehrauli, downloaded on 27 September 2019

Rao, P.R.N., 2017. Water and Heritage: Rejuvenation of Baoli Precincts, Delhi Urban Art Commission,

Tamai, N., Todo, H., Ikemoto, T., 2018. Changes of a Route and an Upstream Well for an Inverted Siphon of Tatsumi Canal in City of Kanazawa, Proceeding of the 21st IAHR-APD Congress 2018, Yogyakarta 2-5 September 2018, Indonesia.

Tatsumi Canal, https://en.wikipedia.org/wiki/Tatsumi_Canal, downloaded on 27 September 2019

The Tatsumi Canal (Falls) in Kanazawa, Ishikawa, Japan. https://commons.wikimedia.org/wiki/Category:Tatsumi_Canal#/media/File:Tatsumi_canal_(Falls).jpg, downloaded on 27 September 2019

Triatmadja. R., Legono, D., Wignyosukarto, B.S., Nurrochmad, F., Sunjoto, S., 2018. Van Der Wijck Irrigation Channel, A Success Story and its Implication, Proceeding of the 21st IAHR-APD Congress 2018, Yogyakarta 2-5 September 2018, Indonesia.

Vishwanath, S., 2010, Know your water heritage, India Water Portal.